Skeletal Radiology (2019) 48:1581–1589
https://doi.org/10.1007/s00256-019-03220-1

SCIENTIFIC ARTICLE

Influence of the ankle position and X-ray beam angulation on the projection of the posterior facet of the subtalar joint

Amy L. Lenz[1] · Nicola Krähenbühl[1] · Kalebb Howell[1] · Rich Lisonbee[1] · Beat Hintermann[2] · Charles L. Saltzman[1] · Alexej Barg[1]

Received: 23 December 2018 / Revised: 4 April 2019 / Accepted: 9 April 2019 / Published online: 27 April 2019

Abstract

Objective Using digitally reconstructed radiographs (DRRs), we determined how changes in the projection angle influenced the assessment of the subtalar joint.

Materials and methods Weightbearing computed tomography (CT) scans were acquired in 27 healthy individuals. CT scans were segmented and processed to create DRRs of the hindfoot. DRRs were obtained to represent 25 different perspectives to simulate internal rotation of the ankle with and without caudal angulation of the X-ray beam. Subtalar joint morphology was quantified by determining the joint space curvature, subtalar inclination angle (SIA), calcaneal slope (CS), and projection of the subtalar joint line on three-dimensional (3-D) reconstructions of the calcaneus.

Results The curvature of the projected joint space was altered substantially over the different DRR projections. Simulated caudal angulation of the X-ray beam with respect to the ankle decreased the SIA and CS significantly. Internal rotation also had a significant impact on the SIA and CS if the X-ray beam was in neutral or in 10° of caudal angulation. An antero-posterior (AP) view of the ankle showed the posterior area of the posterior facet, whereas a more anterior area was visible with internal rotation of the foot and caudal angulation of the X-ray beam.

Conclusion Internal rotation of the foot of 20° is recommended to assess the posterior aspect of the posterior facet, whereas a combined 20° internal rotation of the foot and 40° caudal angulation of the X-ray beam is best to assess the anterior aspect of the posterior facet of the subtalar joint.

Keywords Subtalar joint · Weightbearing CT · Imaging · Anatomy

Introduction

A thorough understanding of the subtalar joint morphology is needed to diagnose pathological conditions of the hindfoot, to develop pre-operative plans for reconstructive surgeries, and to evaluate the success of treatment [1–5]. Recent studies suggested that the posterior facet of the subtalar joint has a significant association in the evolution of hindfoot disorders, including planovalgus deformities and ankle osteoarthritis [2, 3, 5–8]. In addition, the literature has shown that appropriate reduction and fixation of dislocated intra-articular calcaneal and talar fractures are important for a favorable clinical outcome [9]. Thus, there is a clinical need to evaluate the appearance of the posterior facet and the orientation of the subtalar joint relative to other anatomical landmarks of the hindfoot [1, 4, 10]. Radiographic measurements of the subtalar inclination angle (SIA) and calcaneal slope (CS) are often evaluated, in addition to describing the joint space curvature of the posterior facet as being concave, flat, or convex [1, 10, 11]. The SIA is used to interpret inframalleolar compensations resulting from supramalleolar deformities; the CS provides a sense for the subtalar joint orientation in relation to the ground [7, 10–12].

Amy L. Lenz and Nicola Krähenbühl contributed equally to this work

The investigation was performed at the University of Utah, Salt Lake City, USA

✉ Alexej Barg
alexej.barg@hsc.utah.edu

[1] Department of Orthopaedics, University of Utah, 590 Wakara Way, Salt Lake City, UT 84132, USA

[2] Department of Orthopaedics, Kantonsspital Baselland, Rheinstrasse 26, 4410 Liestal, Switzerland

Recently, the general appearance of the posterior facet in addition to the SIA and CS measurements were assessed on weightbearing CT scans [3, 10, 11]. Generally speaking, the SIA and CS were measured in three coronal slices of weightbearing CT scans within the anterior, middle, or posterior regions of the posterior facet [10, 11]. Although weightbearing CT scans have become common for assessment of foot and ankle disorders in recent years, conventional radiographs are still standard for imaging the hindfoot [4]. A formal consensus regarding normative values for these measurements on radiographs has not yet been reached, which has thwarted progress toward standardizing diagnoses based on the evaluation of radiographs.

It has been shown that measurements of the tibio-talar joint, such as the medial distal tibial articular surface angle (TAS), are sensitive to how the foot and X-ray beam are oriented when the film is acquired [13]. Furthermore, current radiographic measurement methods are shown to be sensitive to intra- and inter-observer agreement [14, 15]. The subtalar joint is arguably more complex in shape than the tibio-talar joint, and thus, even subtle changes in the position of the foot, ankle, and X-ray beam are likely to alter the general appearance of this structure and affect measurements of the SIA and CS. However, studies have not assessed how the foot position and orientation of the X-ray beam affect measurements of the subtalar joint in a systematic manner.

The purpose of this study was to determine how changes in the X-ray beam projection angle from horizontal (angulation) and axial rotation of the foot influenced subtalar joint measurements. A second objective was to report SIA and CS measurements in a healthy population to provide a normative dataset for these clinical measurements based on digitally reconstructed radiographs (DRRs). In addition, the subtalar joint line was projected on three-dimensional (3-D) models of the calcaneus to investigate whether the visible area of the posterior facet changes across different foot positions. We hypothesized that the position of the foot and X-ray beam affects accurate evaluation of the subtalar joint on radiographs.

Materials and methods

Participants and data source

Institutional review Board (IRB) approval was obtained to conduct this study. A total of 27 healthy volunteers provided informed consent to participate (Table 1). Inclusion criteria were individuals aged 40–70 years with no history of foot or ankle injury or surgery. Participants with a planovalgus or cavovarus deformity, as observed on radiographs, were excluded. Inclusion and exclusion criteria for each participant were reviewed by a board-certified orthopedic surgeon who was otherwise not involved in the project.

Table 1 Baseline characteristics

Characteristics	Mean (SD; range)
Age (years)	50 (7.3; 40–66)
Gender (male:female; %)	26:74
Side (lef:right; %)	48:52
Height (cm)	169.4 (6.4; 157–180)
Weight (kg)	72.8 (12.4; 57–102)
BMI (kg/m^2)	25.3 (3.8; 18.9–30.4)

BMI body mass index, *SD* standard deviation

Computed tomography acquisition and image processing

Each participant underwent a weightbearing CT scan (Planmed Verity; Planmed Oy, Helsinki, Finland; 0.2-mm slice thickness, 1-mm slice interval) of their foot and ankle with their calcaneus aligned in reference to the second metatarsal for a parallel alignment relative to the scanner's antero-posterior axis. One limb was imaged for each participant to avoid potential issues with statistical testing of nested data. The CT images were segmented to generate 3-D surfaces representing the tibia, fibula, talus, and calcaneus bones (Amira, v6.0.1; Visage Imaging, San Diego, CA, USA). Surfaces were smoothed to reduce segmentation artifact. Next, DRRs of each bone surface were generated by projecting the CT image data to a plane representing the desired view. A total of 25 DRRs were created to represent views with different positions of the foot and radiographic projection angles. Here, we began with an antero-posterior view, defined by no rotation of the foot and no simulated (e.g., the angulation of the DRRs have been changed but not the X-ray equipment) caudal angulation of the X-ray beam (Fig. 1). Iterative combinations of internal rotation of the foot and simulated caudal angulation of the X-ray beam ranging from 0 to 40° (10° increments) yielded the 25 possible permutations; this amounted to a total of 675 DRRs for the cohort (Fig. 2). External rotation of the foot and cranial angulation of the X-ray beam was not assessed because the articular surface of the posterior facet was not clearly visible on those views [4].

General appearance of the posterior facet

For each DRR, the joint space curvature of the subtalar joint posterior facet was classified as convex, flat or concave, as referenced from the calcaneal surface [10]. To do this, DRRs were visualized and calibrated in MATLAB (Version R2017b; MathWorks, Natick, MA, USA) based on a 100-mm line segment output by Amira at the time the DRR was generated.

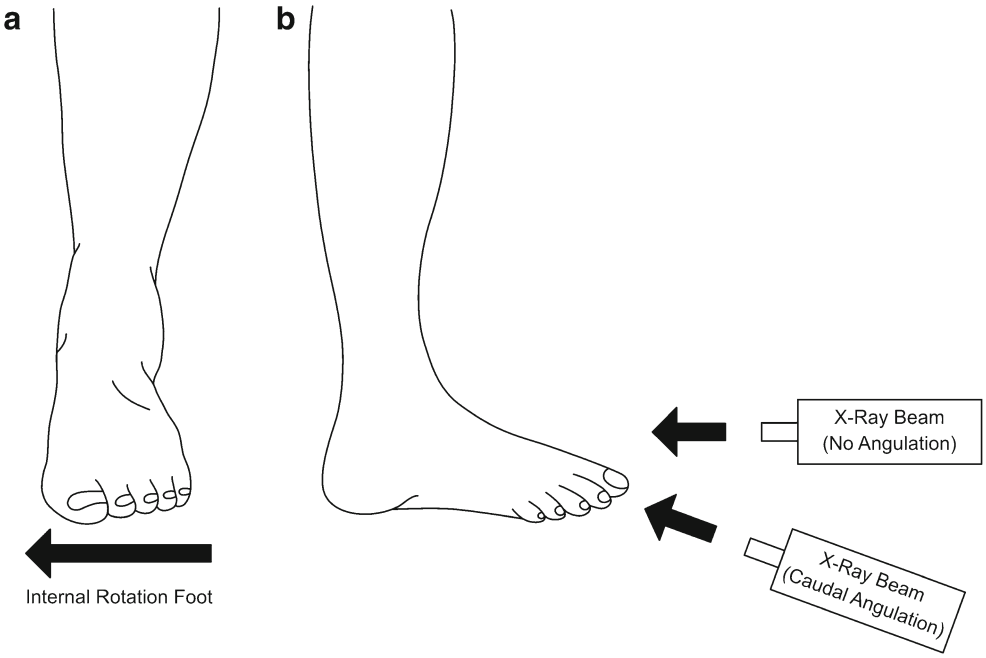

Fig. 1 Illustration of the rotation of the foot and simulated caudal angulation of the X-ray beam. **a** Internal rotation of the foot. **b** Simulated caudal angulation of the X-ray beam

Following calibration, a 120-mm diameter circle was generated within MATLAB to replicate the previously implemented methods of Colin et al. [10]. The user then repositioned the circle over the subtalar joint line visible on the DRR. The curvature of the circle was used as a standardized method to clinically categorize the morphology as convex, flat or concave based on whether the joint line exceeded the curvature of the circle (Fig. 3). The curvature classification was measured at two different times, separated by 2 weeks to assess intra-observer agreement. Measurements obtained by a physician (NK) were compared with those made by a scientist with 1 year of image analysis experience (AL) to establish an estimate of inter-observer agreement.

Radiographic measurements of the subtalar joint

The SIA was measured on each DRR, and was defined as the angle between the surface of the talus and the posterior facet of the calcaneus [1]. The CS was also calculated, and was defined as the angle between a line from the medial to the lateral border of the posterior facet of the calcaneus to a vertical line (Fig. 4) [11]. A custom MATLAB script (Version R2017b; MathWorks, Natick, MA, USA) loaded DRR views individually and guided the reader through measurements of the SIA and CS, automatically calculating angles based on the user input drawn line defining the joint lines. The SIA and CS were measured at two different times, separated by 2 weeks to assess intra-observer agreement. Measurements obtained by a physician (NK) were compared with those made by a scientist (AL) with 1 year of image analysis experience to establish an estimate for inter-observer reliability.

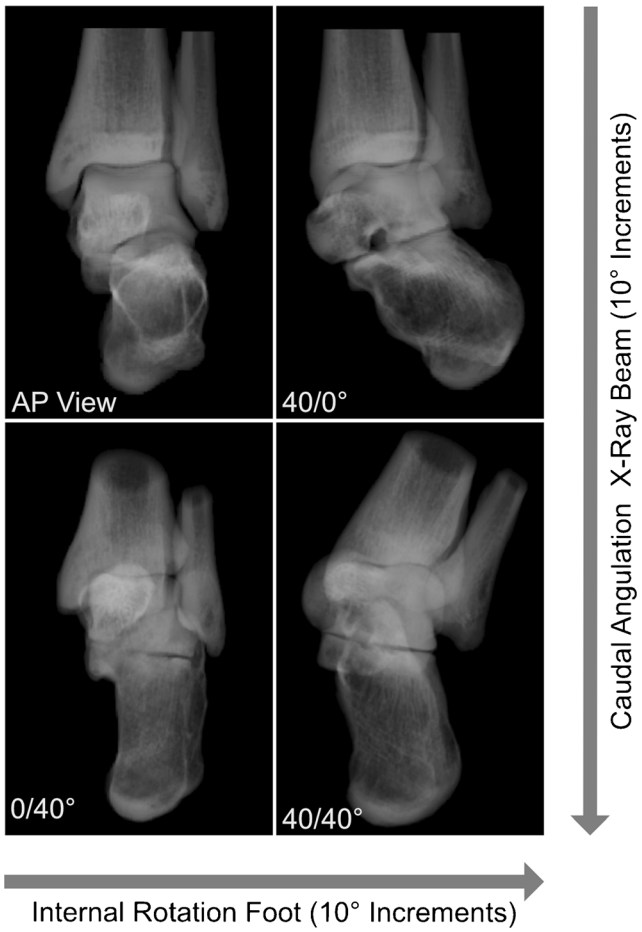

Fig. 2 Starting from an antero-posterior (*AP*) view of the ankle, the digitally reconstructed radiograph (DRR) of the hindfoot was internally rotated to a maximum of 40º (10º increments). Simulated caudal angulation of the X-ray beam was additionally performed

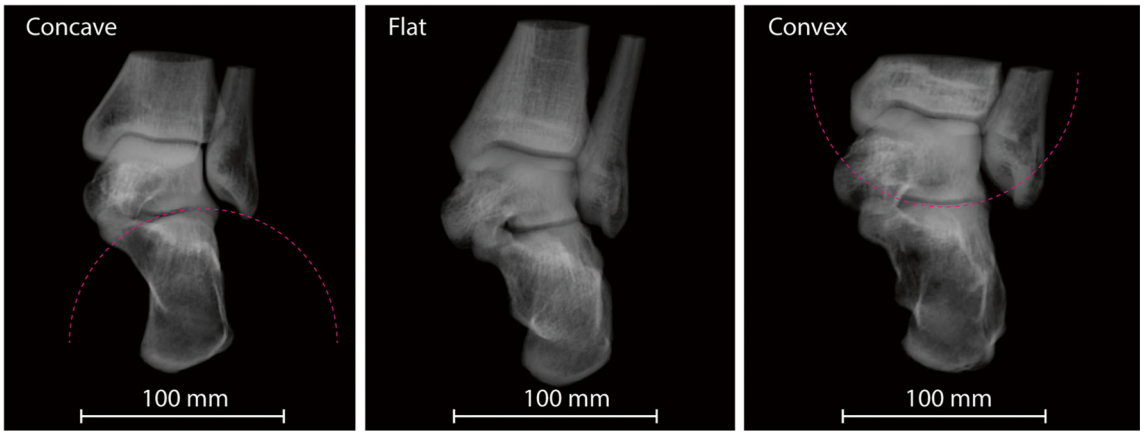

Fig. 3 DRRs from three individual participants in the same DRR projection (20° internal rotation with 10° caudal angulation of the simulated X-ray beam) showing the calibration 100-mm line and a 120-mm diameter half-circle (*dashed*) that was used to clinically categorize the morphology of the posterior facet as being concave (*left*), flat (*center*), or convex (*right*)

Projection of the posterior facet relative to the joint line

The joint line visualized on the DRR views was projected onto the posterior facet and was evaluated by defining virtual anatomical landmarks around the perimeter of the articular surface (Fig. 5). First, six anatomical landmarks of the posterior facet of the subtalar joint (calcaneal side) were defined in the CT image data as virtual beads and included the antero-medial, medial, posterior, superior, lateral, and antero-lateral points. The position of these virtual beads was defined mathematically. First, the boundary of the ridge representing the articular surface of the posterior facet was defined by visualizing the second principle of curvature on the segmented 3-D bone reconstructions representing the calcaneus (PostView, v2.1.0; FEBio, Salt Lake City, UT, USA). Each calcaneus was aligned in reference to the second metatarsal before the virtual beads were placed. The six anatomical bead locations were mathematically placed based on second principle curvature for the nodal locations within the bone's reconstruction identified by the ridge of the articular surface; this ensured consistency in the placement of the virtual beads. Placement of the virtual beads was checked by a physician (NK) to ensure that placement was clinically and anatomically accurate. Once the bead locations were established, their placement was used to quantify the direction and magnitude of anatomical bead locations surrounding the posterior facet relative to the visualized joint line in each of the 25 DRR views. A rotation sequence for the appropriate internal rotation and simulated caudal angulation of the X-ray equipment was applied to each 3-D calcaneus model containing the defined anatomical beads. The 3-D model was then calculated as a projection onto the plane of an equivalent 2-D DRR view in which a physician (NK) selected the points defining the joint line formerly identified for the CS calculation. The custom MATLAB script used the points to perform a curve fit of the joint line in that projection view and sequentially calculated the direction and magnitude of the six anatomical beads from the joint line within the calcaneal articular surface based on nodes within the 3-D surface model.

Statistical analysis

Inter- and intra-observer agreement for joint space curvature classification were assessed using unweighted Cohen's kappa for categorical variables across observers and weighted Cohen's kappa statistics for within an

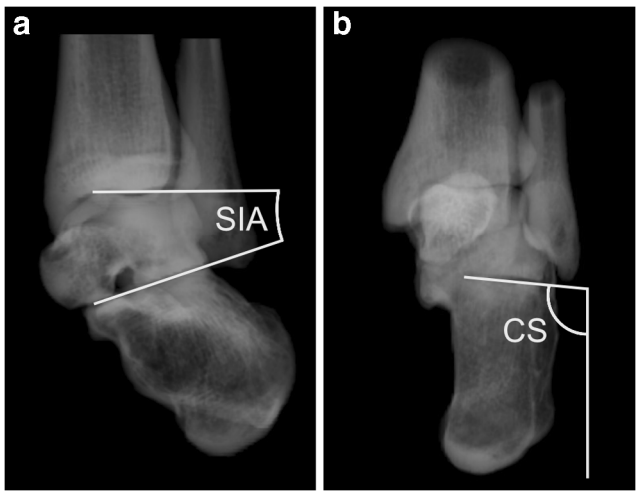

Fig. 4 Subtalar joint alignment assessment. **a** DRR showing the hindfoot at 40° internal rotation (without simulated caudal angulation of the X-ray beam). The subtalar inclination angle (*SIA*) was defined as the angle between the talar surface and the surface of the posterior facet of the subtalar joint. **b** DRR showing neutral rotation of the hindfoot with 40° caudal angulation. The calcaneal slope (*CS*) was defined as the angle between the posterior facet of the subtalar joint to a line vertical to the ground

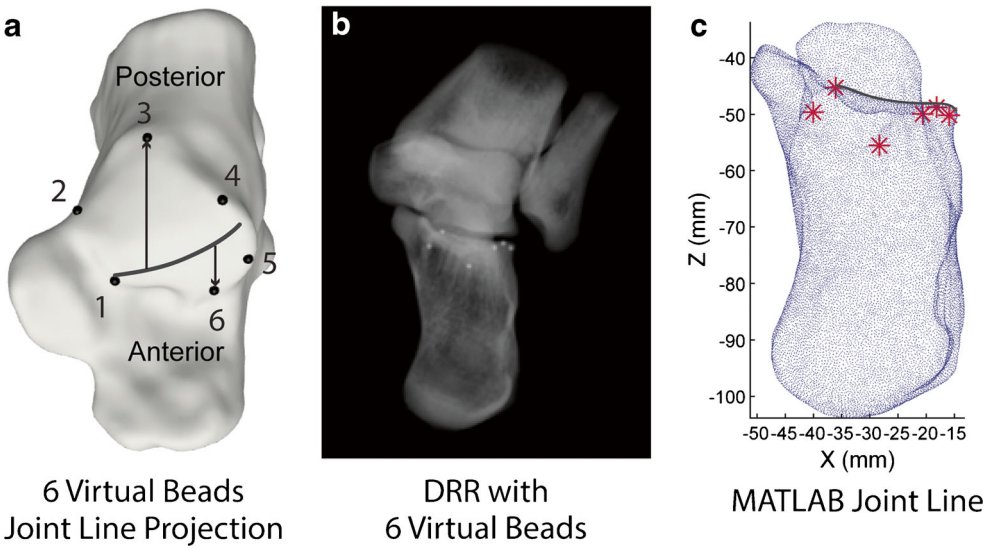

Fig. 5 Flow chart outlining the computational process for placing virtual beads and projecting the joint line onto the articular surface of the posterior facet. **a** Six virtual bead locations were placed around the perimeter of the posterior facet. **b** DRR projection (30º of ankle internal rotation and 40° of simulated caudal angulation of the X-ray beam) with six virtual beads. **c** MATLAB figure of calcaneus rotated into the 30/40° position; the *black joint line* was defined as a curve fit, with the *red stars* representing the six virtual bead locations

observer's ratings [16]. Agreement was considered to be almost perfect for a K > 0.81; substantial agreement with a K = 0.61–0.80; moderate agreement with a K = 0.41–0.60; fair agreement with a K = 0.21–0.40; and slight agreement with a K < 0.20 [16]. Inter- and intra-observer agreement were assessed using the two-way random intraclass correlation coefficient (ICC) and presented with a 95% confidence interval (95% CI) for SIA and CS measurements. Agreement was considered to be very good for an ICC > 0.80; good with an ICC = 0.61–0.80; moderate with an ICC = 0.41–0.60; fair with an ICC = 0.21–0.4; and poor with an ICC < 0.20 [17]. To test for differences in the SIA and CS between the baseline AP view, represented as (0.0°) to define 0° of internal rotation and 0° of simulated caudal angulation of the X-ray equipment, and either the influence of internal rotation or caudal angulation separately in 10° increments, Student's *t* tests were used. Statistical significance was set as $p < 0.05$. MATLAB and IBM SPSS Statistics Version 25.0 (Armonk, NY, USA) was used for statistical analyses.

Results

General appearance of the posterior facet

The joint space curvature of the subtalar joint posterior facet of the calcaneus changed between different viewing perspectives. On the AP view of the foot and ankle, the posterior facet appeared convex on each DRR (Fig. 6). With further internal rotation of the foot, the percentage of flat-shaped posterior facets increased, reaching the highest portion with 77.8% at internal rotation of 30°. At 30 and 40° internal rotation, concave posterior facets were additionally evident (18.5% at 30 and 40.7% at 40° of internal rotation). None of the posterior facets showed a convex shape at 40° internal rotation. 11.1% of the posterior facets showed a flat morphology when the X-ray equipment was angulated 10° caudally without internal rotation (Fig. 6). With further caudal angulation, the percentage of feet showing a flat posterior facet increased, reaching 63.0% at 40°. None of the posterior facets were convex at a caudal angulation of 40° (neutral rotation), but 37.0% showed

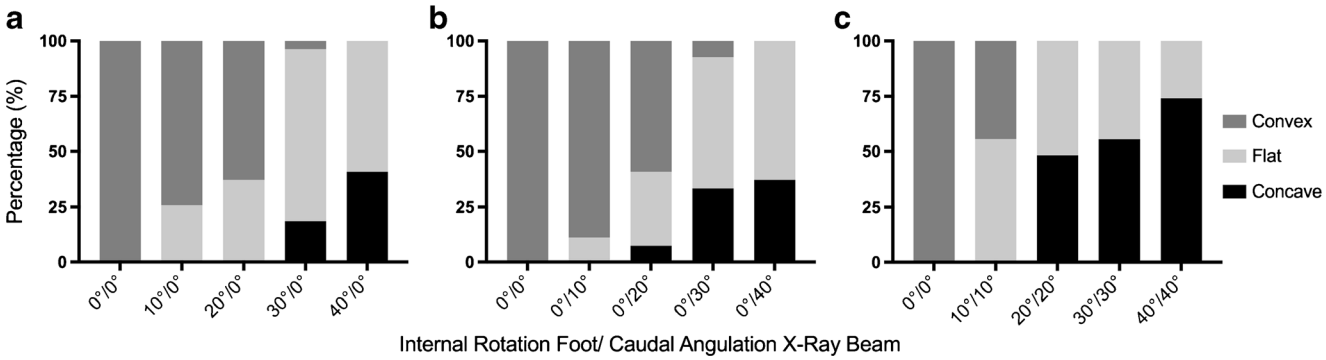

Fig. 6 Impact of internal rotation of the foot and simulated X-ray beam angulation on the joint space curvature morphology of the subtalar joint. **a** The morphology was dependent on the rotation alone and **b** isolated simulated caudal angulation of the X-ray beam with respect to the foot. **c** A combination of equal rotation and caudal angulation of the X-ray equipment shifted the visualization from convex- to more concave-dominated visualization

Table 2 Impact of the simulated X-ray beam angulation on the subtalar inclination angle (*SIA*) radiographic measurement of the posterior facet of the subtalar joint

SIA		Internal rotation									
		0°		10°		20°		30°		40°	
		Mean (SD)	*p* value	Mean (SD)	*p* value	Mean (SD)	*p* value	Mean (SD)	*p* value	Mean (SD)	*p* value
Caudal angulation	0°	12.0 (6.1)	–	14.0 (6.3)	–	18.2 (5.6)	–	20.5 (5.5)	–	20.9 (5.3)	–
	10°	9.9 (5.9)	0.132	12.4 (6.0)	0.028*	14.4 (5.1)	<0.001*	15.3 (4.7)	<0.001*	15.2 (4.9)	<0.001*
	20°	8.7 (5.3)	0.009*	9.0 (5.8)	<0.001*	9.2 (5.1)	<0.001*	9.5 (4.8)	<0.001*	9.9 (5.3)	<0.001*
	30°	4.4 (2.7)	<0.001*	4.5 (3.3)	<0.001*	4.4 (3.1)	<0.001*	5.0 (3.4)	<0.001*	5.5 (4.7)	<0.001*
	40°	3.8 (3.4)	<0.001*	3.6 (2.8)	<0.001*	3.8 (3.1)	<0.001*	4.4 (3.5)	<0.001*	4.3 (3.3)	<0.001*

*Indicates statistical significance ($p < 0.05$) between 0° caudal angulation and 10, 20, 30, and 40° caudal angulation

a concave morphology. A similar trend was evident for other positions of the foot and X-ray beam (e.g., when the foot was 10° internally rotated and the X-ray beam 10° caudally angulated, etc.): combination of equal rotation and caudal angulation shifted the visualization from convex- to more concave-dominated visualization. Inter- and intra-observer agreement for classifying joint space curvature differed across the DRR views. Four DRR perspectives (0/0, 0/10, 20/0, and 40/0; internal rotation/caudal angulation) had a K range of 0.61–1, indicating substantial to almost perfect agreement for both inter- and intra-observer reliability. Overall for inter-observer Kappa values, the reliability ranged from 0.198 to 1. Intra-observer agreement across viewing perspectives ranged from 0.275 to 1.

Radiographic measurements of the subtalar joint

Across the 25 DRR viewing perspectives, SIA measurements ranged on average from 3.8 to 20.9° (Table 2) and CS measurements ranged on average from 54.8 to 105.8° (Table 3). Simulated caudal angulation of the X-ray beam decreased the mean SIA significantly, except for one DRR view with 10° caudal angulation at neutral rotation ($p = 0.132$, Table 2). For CS measurements, caudal angulation significantly influenced all measurements compared with a baseline internal foot rotation ($p \leq 0.03$, Table 3). The mean SIA and CS also changed when the foot was internally rotated compared with a constant simulated beam angulation (Table 4). Specifically, a significant decrease (compared with the antero-posterior view) was evident at 10–40° internal rotation for neutral and 10° simulated caudal angulation (Table 4). Internal rotation of the foot did not have a significant impact on the SIA and CS measurements if the simulated X-ray beam angulation was 20–40° caudally. Inter- and intra-observer agreement for measuring the SIA and CS differed across the various DRR views. The lowest values were evident at the antero-posterior view of the foot without any caudal angulation (SIA inter-observer agreement 0.368 and intra-observer agreement 0.806, CS inter-observer agreement 0.184 and intra-observer agreement 0.833). For the other views, the reliability ranged from 0.416 to 0.967 (SIA) and from 0.586 to 0.996 (CS).

Projection of the joint line onto the posterior facet

The visible area where the joint line was projected onto the posterior facet changed between the different viewing

Table 3 Impact of the simulated X-ray beam angulation on the calcaneal slope (*CS*) radiographic measurement of the posterior facet of the subtalar joint posterior facet

CS		Internal rotation									
		0°		10°		20°		30°		40°	
		Mean (SD)	*p* value	Mean (SD)	*p* value	Mean (SD)	*p* value	Mean (SD)	*p* value	Mean (SD)	*p* value
Caudal angulation	0°	98.4 (6.2)	–	100.5 (6.3)	–	104.3 (5.7)	–	106.1 (4.8)	–	105.8 (4.7)	–
	10°	95.4 (6.3)	0.030	97.9 (6.4)	<0.001*	99.9 (5.5)	<0.001*	100.6 (4.2)	<0.001*	99.6 (4.5)	<0.001*
	20°	93.8 (6.3)	0.001	94.4 (6.4)	<0.001*	84.3 (5.6)	<0.001*	84.3 (4.8)	<0.001*	94.1 (5.3)	<0.001*
	30°	88.1 (5.7)	**<0.001***	87.9 (5.7)	<0.001*	88.4 (5.2)	<0.001*	88.2 (5.7)	<0.001*	89.1 (5.7)	<0.001*
	40°	84.5 (5.3)	**<0.001***	84.5 (5.5)	<0.001*	84.0 (5.1)	<0.001*	84.2 (5.1)	<0.001*	54.8 (6.0)	<0.001*

*Indicates statistical significance ($p < 0.05$) between 0° caudal angulation and 10, 20, 30, and 40° caudal angulation

Table 4 Impact of internal rotation of the foot on the SIA and CS

			Internal rotation foot			
			10° *P* value	20°	30°	40°
Caudal angulation X-ray beam	SIA	0°	0.085	*<0.001	*<0.001	*<0.001
		10°	0.080	*<0.001	*<0.001	*<0.001
		20°	0.745	0.564	0.300	0.158
		30°	0.870	0.897	0.259	0.217
		40°	0.538	0.909	0.113	0.427
	CS	0°	0.068	*<0.001	*<0.001	*<0.001
		10°	0.060	*<0.001	*<0.001	*<0.001
		20°	0.604	0.630	0.584	0.729
		30°	0.567	0.532	0.778	0.123
		40°	0.755	0.200	0.410	0.497

*Indicates statistical significance ($p < 0.05$) of 0° internal rotation (foot) vs 10/20/30/40° internal rotation (foot)

perspectives (Fig. 7). Although on an AP view of the foot and ankle the posterior area of the posterior facet was visible, a slightly more anterior area was visible when the foot was internally rotated. Simulated caudal angulation of the X-ray beam also changed the visible area of the posterior facet from posterior (without caudal angulation) to more anterior (40° caudal angulation). Internal rotation of the foot only had a minimal effect on the distance from the posterior-most point marked on the posterior facet (3-D models) to the projected subtalar joint line on DRRs (Fig. 8). An increase in the distance was evident with internal rotation of the foot combined with a 20° caudal angulation. A similar pattern was evident for the anteromedial-most point (Fig. 8) with the difference that those points were located anterior to the joint line in most views.

Discussion

The influence of various DRR projection views with different internal rotations of the foot and simulated caudal angulation of X-ray equipment on the visualization of the subtalar joint was assessed. Our hypothesis was confirmed, the position of the foot affects the radiographic appearance and visible area of the posterior facet on DRRs. The three major findings were:

1. Increasing internal rotation of the ankle or increasing caudal angulation of the X-ray beam shifted the projected subtalar joint morphology from primarily convex to flat; however, simultaneously increasing both internal rotation and caudal tilt shifted the projected joint morphology from primarily convex to concave.
2. Measurements describing the alignment of the subtalar joint (SIA and CS) changed between different viewing perspectives with internal rotation not having an influence after 20° of caudal angulation of the X-ray beam.
3. Changes in the DRR projection visualized a joint line on different aspects of the articulating surface of the posterior facet.

Understanding the radiographic appearance of the posterior facet in healthy individuals on DRRs is important to identify pathological changes among symptomatic, diseased ankles.

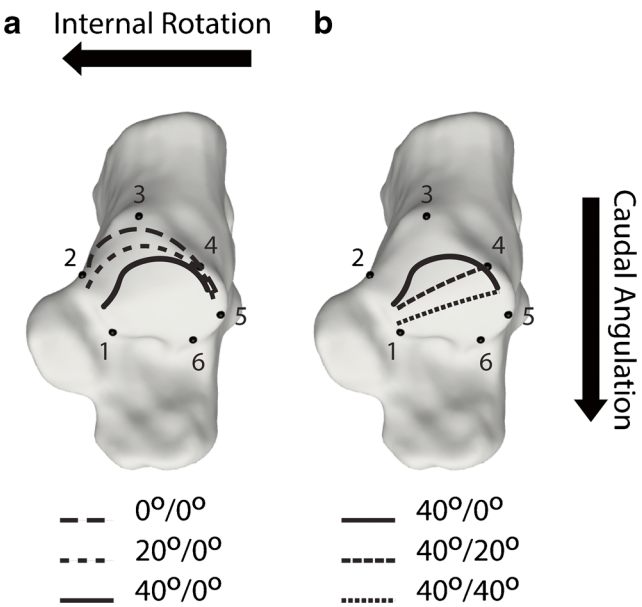

Fig. 7 Projection of the posterior facet on 3-D models of the calcaneus. Points *1–6* show the anatomical landmarks of the posterior facet. **a** Internal rotation (without caudal angulation of the X-ray beam) demonstrates a curved joint line projected onto the posterior facet, the visualized joint line begins posteriorly and moves anteriorly. **b** Simulated caudal angulation (at 40° internal rotation) of the X-ray beam shows a more anterior aspect of the posterior facet of the subtalar joint

Studies using weightbearing CT scans have shown that the configuration of the posterior facet may have an impact on the evolution of ankle osteoarthritis (e.g., slower or faster progression of the degenerative changes) [7, 11]. Other studies using weightbearing CT scans showed that the slope of the posterior facet is more valgus for patients suffering from flatfoot deformities compared with healthy ankles [7, 11]. However, well-controlled DRRs generated from the gold standard of weightbearing CT scans had not been assessed to evaluate how changes in the alignment of the X-ray beam could affect visualization of the subtalar joint, which provided the impetus for this study.

A thorough understanding of the radiographic appearance of the posterior facet is important for correct interpretation of intra-operative fluoroscopy and post-operative radiographs following reconstructive surgery of the hindfoot (e.g., after fixation of intra-articular calcaneal or talus fractures). For example, overlooking malreduction at the level of the posterior facet leads to rapid degeneration of the subtalar joint [9]. Additional surgeries such as a calcaneal osteotomy or corrective subtalar fusion may be necessary in those patients. A more accurate assessment of the posterior facet is possible if the radiographic appearance is understood in depth, which is provided in this study.

Recent studies using single coronal CT images under weightbearing conditions showed that the morphology and configuration of the posterior facet varies between healthy individuals [10]. A convex morphology (calcaneal side) was evident in 88%, whereas 12% showed a flat morphology [10]. In addition, the configuration of the posterior facet changed from anterior (neutral orientation) to posterior (varus orientation) [10]. Using DRRs, the morphology of the posterior facet was dependent on the viewing perspective. On the AP view, the morphology was convex in each DRR, whereas with internal rotation or simulated caudal angulation of the X-ray beam, the percentage of a flat or convex morphology increased. Therefore, it seems likely that inter-individual differences in the appearance of the posterior facet on CT is based on the rotation of the foot. Findings of the configuration of the posterior facet on DRRs are comparable with the results on weightbearing CTs: caudal angulation (showing the anterior aspect of the posterior facet) of the foot was associated with a more neutral orientation of the posterior facet in the coronal plane, whereas the orientation was more varus when the foot was in a plantigrade position (showing the posterior aspect of the posterior facet) [7]. Of note, the configuration of the posterior facet assessed on DRRs was dependent on the viewing perspective (e.g., internal rotation of the foot and simulated caudal angulation of the X-ray beam had an impact on the joint configuration).

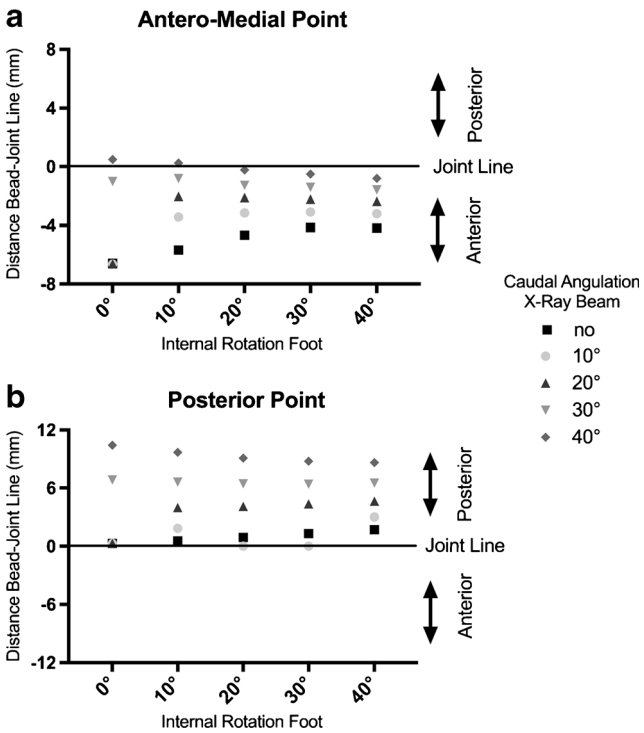

Fig. 8 Distance between **a** the antero-medial-most and **b** posterior-most points of the posterior facet to the projected subtalar joint line on DRRs

Each viewing perspective differed in terms of the projected joint curvature, alignment (SIA and CS), and visible area of the posterior facet. Previous research has shown that the joint axis of the posterior facet of the calcaneus is slightly externally rotated [18, 19]. Therefore, a slight internal rotation of the foot while radiographs are acquired provides a more perpendicular view of the posterior facet. Of note, our radiographic measurements (SIA and CS) describing the configuration of the posterior facet showed a poor reliability on the antero-posterior view, but increased when the foot was internally rotated. The subtalar joint is barely visible in an antero-posterior view, maybe explaining the insufficient reliability of this view. Consequently, a 20° internal rotation of the foot is recommended to assess the posterior aspect of the posterior facet, whereas a combined 20° internal rotation (foot) and 40° caudal angulation of the X-ray beam is ideal for assessment of the anterior aspect of the posterior facet. If the foot is internally rotated 20°, the projected subtalar joint morphology (e.g., convex vs flat vs concave) can additionally be reliably assessed. This is important as the identification of the subtalar joint morphology is not reliable for most other views. Multiple radiographs can easily be acquired intra-operatively using fluoroscopy. Using standard X-ray equipment, this approach may be not suitable. Use of DRRs that are derived from weightbearing CT images is advantageous, as it allows for computer-controlled projections to be constructed, thus preventing errors that would be present if standard X-ray equipment had been used for this study.

This study has several limitations. First, DRRs were used for assessment of the posterior facet. Although previous research has shown that measurements on DRRs assessing the

alignment of the ankle joint are comparable with measurements on radiographs [20]. However, measurements performed at the level of the subtalar joint may differ between DRRs and radiographs. Second, intraoperative assessment of the subtalar joint during reconstructive surgery is done with the patient supine or prone, not in a weightbearing condition, as was the case for the CT images utilized. Application of load may have an impact on the appearance of the posterior facet. Third, only healthy individuals were included in this study. The posterior facet in diseased ankles may show a different radiographic appearance.

To conclude, the position of the foot has an impact on the radiographic appearance and the visible area of the posterior facet on DRRs. Twenty degrees of internal rotation of the foot is recommended to assess the posterior aspect of the posterior facet, whereas a combined 20° internal rotation of the foot and 40° caudal angulation of the X-ray beam is best to assess the anterior aspect of the posterior facet of the subtalar joint. A thorough understanding of the projection of the subtalar joint in different positions of the foot is important for a meaningful interpretation of the hindfoot on conventional radiographs.

Acknowledgments The authors thank Andrew E. Anderson, PhD, research associate professor at the University of Utah, who provided technical and editorial support.

Funding This work was supported by a grant from the Swiss Society of Orthopaedic Surgery (Swiss Orthopaedics). It was also supported by the LS Peery Foundation (University of Utah) and by the National Institutes of Health (NIH-R21AR063844). Nicola Krähenbühl received a grant from the Swiss National Science Foundation (SNF; grant number P2BSP3_174979).

Compliance with ethical standards

Ethical approval All procedures performed in studies involving human participants were in accordance with the ethical standards of the institutional and/or national research committee and with the 1964 Declaration of Helsinki and its later amendments or comparable ethical standards.

References

1. Krähenbühl N, Horn-Lang T, Hintermann B, Knupp M. The subtalar joint: a complex mechanism. EFORT Open Rev. 2017;2(7):309–16.
2. Cody EA, Williamson ER, Burket JC, Deland JT, Ellis SJ. Correlation of talar anatomy and subtalar joint alignment on weightbearing computed tomography with radiographic flatfoot parameters. Foot Ankle Int. 2016;37(8):874–81.
3. Wang B, Saltzman CL, Chalayon O, Barg A. Does the subtalar joint compensate for ankle malalignment in end-stage ankle arthritis? Clin Orthop Relat Res. 2015;473(1):318–25.
4. Lopez-Ben R. Imaging of the subtalar joint. Foot Ankle Clin. 2015;20(2):223–41.
5. Apostle KL, Coleman NW, Sangeorzan BJ. Subtalar joint axis in patients with symptomatic peritalar subluxation compared to normal controls. Foot Ankle Int. 2014;35(11):1153–8.
6. Hayashi K, Tanaka Y, Kumai T, Sugimoto K, Takakura Y. Correlation of compensatory alignment of the subtalar joint to the progression of primary osteoarthritis of the ankle. Foot Ankle Int. 2008;29(4):400–6.
7. Krähenbühl N, Tschuck M, Bolliger L, Hintermann B, Knupp M. Orientation of the subtalar joint: measurement and reliability using weightbearing CT scans. Foot Ankle Int. 2016;37(1):109–14.
8. Probasco W, Haleem AM, Yu J, Sangeorzan BJ, Deland JT, Ellis SJ. Assessment of coronal plane subtalar joint alignment in peritalar subluxation via weight-bearing multiplanar imaging. Foot Ankle Int. 2015;36(3):302–9.
9. Rammelt S, Bartonicek J, Park KH. Traumatic injury to the subtalar joint. Foot Ankle Clin. 2018;23(3):353–74.
10. Colin F, Horn Lang T, Zwicky L, Hintermann B, Knupp M. Subtalar joint configuration on weightbearing CT scan. Foot Ankle Int. 2014;35(10):1057–62.
11. Krähenbühl N, Siegler L, Deforth M, Zwicky L, Hintermann B, Knupp M. Subtalar joint alignment in ankle osteoarthritis. Foot Ankle Surg. 2019;25(2):143–9..
12. Van Bergeyk AB, Younger A, Carson B. CT analysis of hindfoot alignment in chronic lateral ankle instability. Foot Ankle Int. 2002;23(1):37–42.
13. Barg A, Amendola RL, Henninger HB, Kapron AL, Saltzman CL, Anderson AE. Influence of ankle position and radiographic projection angle on measurement of supramalleolar alignment on the anteroposterior and hindfoot alignment views. Foot Ankle Int. 2015;36(11):1352–61.
14. Guo C, Zhu Y, Hu M, Deng L, Xu X. Reliability of measurements on lateral ankle radiographs. BMC Musculoskelet Disord. 2016;17:297.
15. Kuo CC, Lu HL, Lu TW, Lin CC, Leardini A, Kuo MY, et al. Effects of positioning on radiographic measurements of ankle morphology: a computerized tomography-based simulation study. Biomed Eng Online. 2013;12:131.
16. Hallgren KA. Computing inter-rater reliability for observational data: an overview and tutorial. Tutor Quant Methods Psychol. 2012;8(1):23–34.
17. Yeung TW, Chan CY, Chan WC, Yeung YN, Yuen MK. Can preoperative axial CT imaging predict syndesmosis instability in patients sustaining ankle fractures? Seven years' experience in a tertiary trauma center. Skeletal Radiol. 2015;44(6):823–9.
18. Broden B. Roentgen examination of the subtaloid joint in fractures of the calcaneus. Acta Radiol. 1949;31(1):85–91.
19. Sarrafian SK. Biomechanics of the subtalar joint complex. Clin Orthop Relat Res. 1993;290:17–26.
20. Barg A, Bailey T, Richter M, de Cesar Netto C, Lintz F, Burssens A, et al. Weightbearing computed tomography of the foot and ankle: emerging technology topical review. Foot Ankle Int. 2018;39(3):376–86.